A parabolic mirror can be effectively defocused changing the incidence angle pitch angle [RD4], thereby overcoming the limited travel range in the detector stage. In Figure 8, we show the result of the defocusing by reducing the incidence angle by 20 arcmin, and moving the detector extrafocal by 150 mm. The mirror remains defocused within the field of view of TRoPIC, and the intensity exhibits closely spaced, parallel striations. Due to the reduction of the incidence angle, the focus has moved so farther away that, even with the extrafocal shift imparted, rays do not cross each other and striations do not overlap. Hence, the intensity modulations are connected to the residual pattern of mid-frequencies in the error shape map of the mirror surface [RD10]. In fact, a simulation from the mirror metrology, in the same defocusing configuration, returns a virtually identical intensity distribution. The only remarkable difference is a faint halo of scattered rays on the two side of the arc, which can be explained assuming that, with the mirror at a smaller incidence angle like this, some rays through the entrance slit illuminate also regions out of the optically-polished area. The same comments apply to an intrafocal image at -12 arcmin pitch angle alignment (Figure 9). The intensity modulations can still be accurately explained by the current metrology dataset, with the exception of the faint scattering halo.

3. Uncoated mirror under parallel X-ray beam (1.49 keV)

3.1. Alignment in X-rays

After the insertion of the ZP to make the incident beam parallel, the mirror had to be realigned in order to have the 1st order of the ZP on the paraboloid axis. Since the ZP is located on the Wald side at a 162 mm distance from the optical axis of the PANTER tube and sends the 1st order beam to a direction parallel to the axis, it deviates the beam by 162 mm / 125 m = 4.4 arcmin, the mirror should be re-oriented in the pitch angle by the same amount. In practice, the mirror has been re-aligned on the PANTER axis, set at the correct angle for the diverging beam setup, then translated by 162 mm to the Wald side without changing the alignment drastically, which in turn enables an easy location of the correct diffraction order, the only one that is *stigmatic* and *focused* when the detector distance is set near 4960 mm. The alignment was subsequently refined in yaw, pitch (Figure 10) and distance, using the method already adopted for the diverging beam setup [RD4].

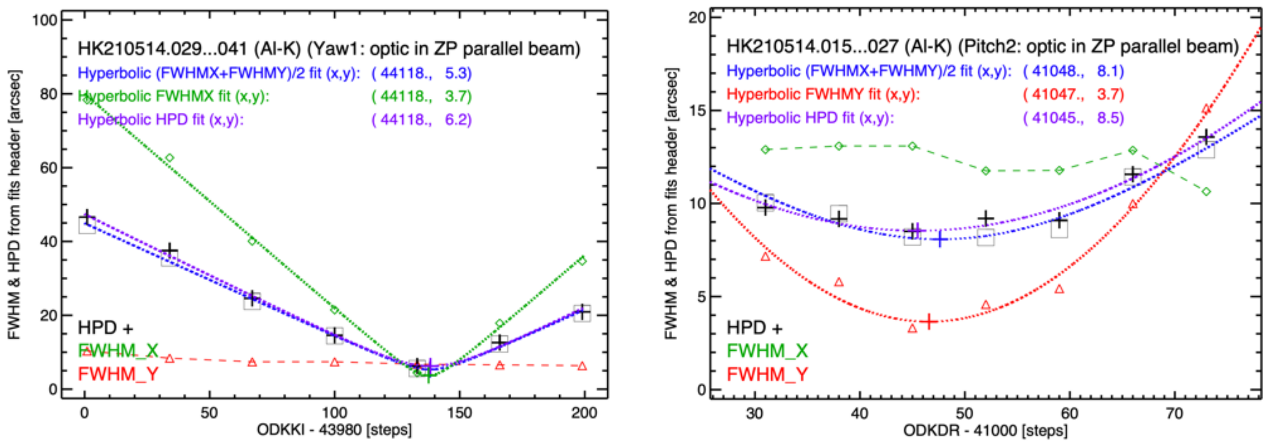

Figure 10: rough focus search in parallel beam with TRoPIC. Left: yaw scan. Right: pitch scan. The focal distance was not optimized yet.

At the pitch angle that minimizes the HEW, the optimal detector distance (Figure 11 and Figure 12), was found with TRoPIC 196 mm intra-focal (DETQK 154400) wrt the best diverging focus, as anticipated in Sect. 2.2. The measurement with PIXI (Figure 15) yields a focal length that is 5 mm longer. This remains within the ± 5 mm uncertainty found on these measurements.

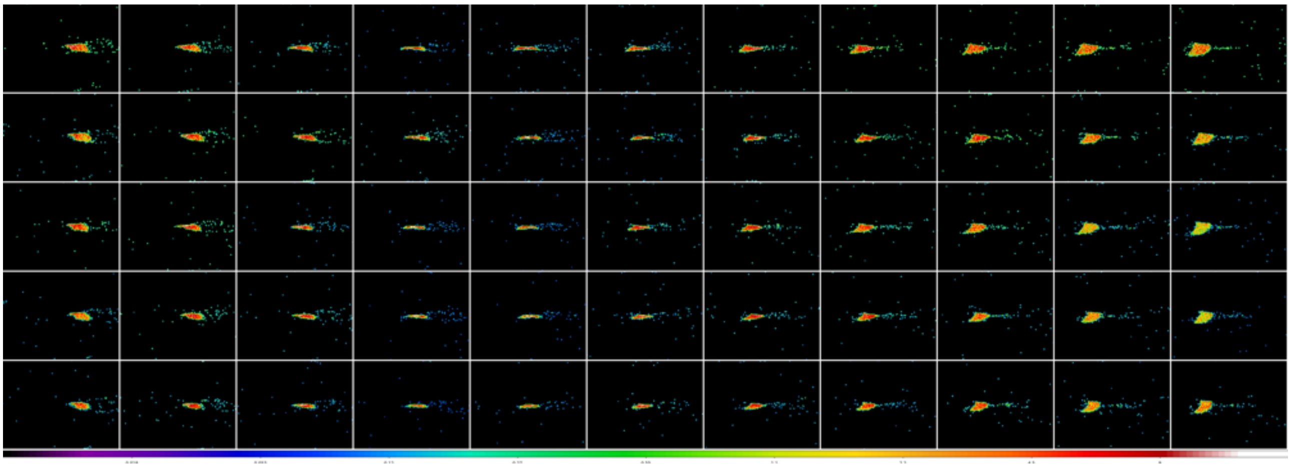

Figure 11: coarse focus search in parallel beam with TRoPIC. Rows: variation with the detector distance. Columns: variation with the pitch angle with 0.5 arcmin steps. Nearby rows are mutually shifted by 45 mm in reality.

3.2. The TRoPIC view

The HEW measurement with TRoPIC in the best focus (Figure 12) returned the same difficulties encountered with the diverging beam, because the PSF is strongly peaked and a single pixel of TRoPIC covers a HEW. A PSF cannot be traced with certainty, but the **HEW does not exceed 3.14 arcsec**: in fact, 51% of all collected photons are found within a 40 µm angular radius. This result is well aligned with the predicted value of **3.3 arcsec** expected from the shape and error metrology, and assuming a 1.6 arcsec X-ray source.

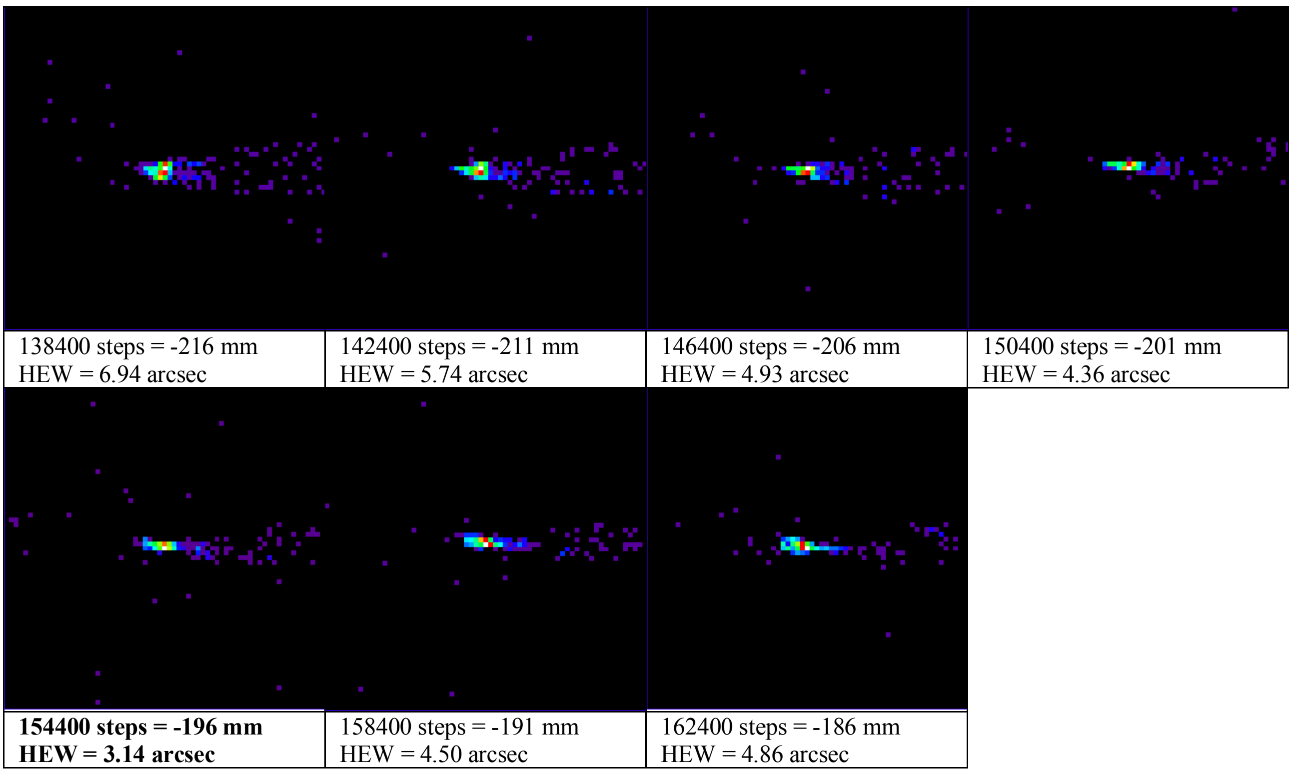

Figure 12: focus search in parallel beam setup at 1.49 keV with TRoPIC, varying the detector distance from intra- to extra-focal. The steps are those of the DETQK stage.

Actually, *the expected value is probably overestimated because the X-ray source is much smaller than we have assumed* (< 0.7 arcsec); even so, the HEW obtained from the simulation (Figure 13) remains almost unchanged as dominated by the TRoPIC pixel size. We can therefore set 3.14 arcsec as *upper limit to the angular resolution HEW of the BEaTriX mirror.* An interesting comparison of the best focus with TRoPIC vs. the simulation from metrology and the reduced source is shown in Figure 13. The asymmetry in the scattering in the experimental image could not be reproduced in the simulation.

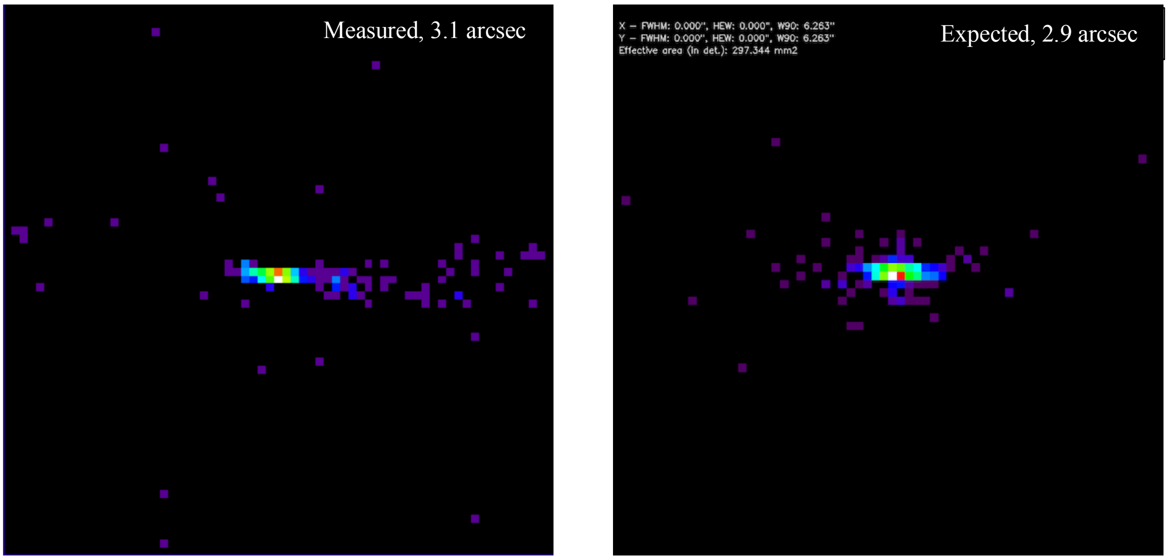

Figure 13: the best focus of the BEaTriX mirror seen by TRoPIC at 1.49 keV, in parallel beam setup. Left: measured. Right: simulated from metrology.

3.3. The PIXI view

A better oversampling of the PSF can be obtained with PIXI, that has higher spatial resolution (20 µm) despite the higher background level. The best focus search yields a best focal length 201 mm intrafocal wrt the diverging focus position (Figure 15).

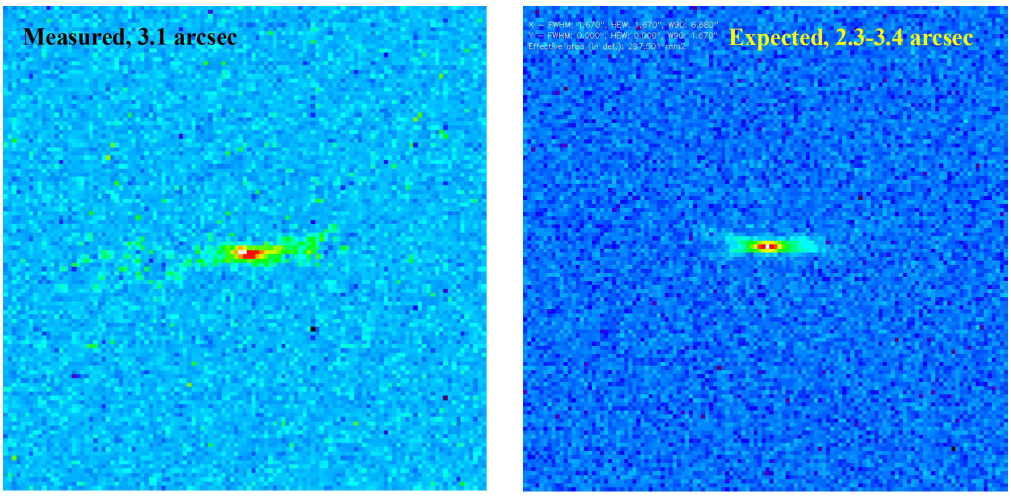

Figure 14: the best focus of the BEaTriX mirror seen by PIXI at 1.49 keV, in parallel beam setup. Left: measured. Right: simulated from metrology. The uncertainty comes from the variable level of background assumed in the simulation.

Again, this agrees with the measurement done with TRoPIC (Figure 12) within a 5 mm error margin. The best focus also yields a HEW in agreement with TRoPIC. In the absence of a fluctuating background, the expected HEW with the real size of the source and the PIXI pixel would be 2.3 arcsec at 1.49 keV. Indeed, the pixel size is still on the order of 1 arcsec and the background introduces some uncertainty, so the 3 arcsec HEW measured at 1.49 keV should be retained as an upper limit (Figure 14). Nevertheless, the measurement with PIXI is valuable information, as it provides an independent confirmation of the results seen with TRoPIC.

A deep exposure in focus is shown in Figure 16; the prevalent, albeit faint, scattering on the right side cannot be understood easily. It might be, for example, due to illumination on the very edge of the polished area, which could have a worse optical quality. The effect seems to be, anyway, very small. Other details can be found in the report issued by the PANTER team [RD11].

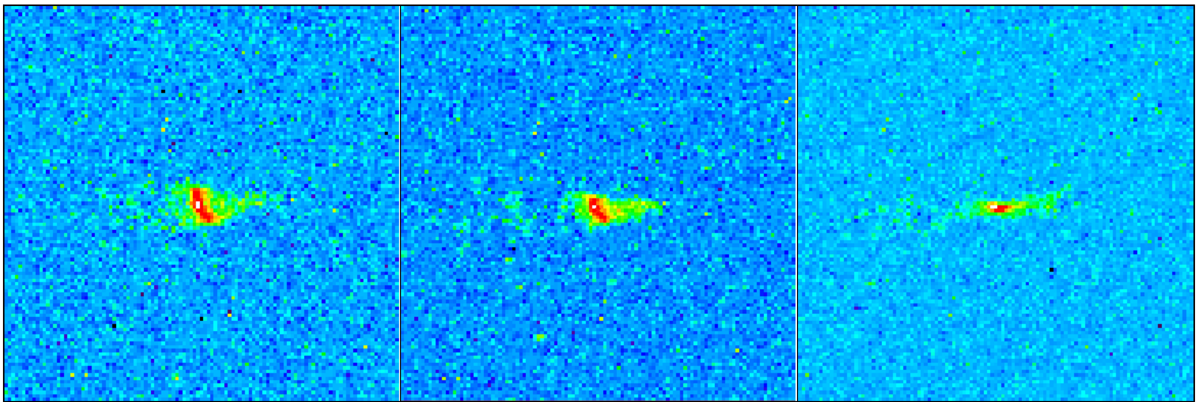

DETQK 138341 steps = -216 mm FWHM x = 3.35 arcsec FWHM y = 6.48 arcsec HEW = 5.56 arcsec	DETQK 142341 steps = -211 mm FWHM x = 3.43 arcsec FWHM y = 4.42 arcsec HEW = 4.99 arcsec	**DETQK 150341 steps = -201 mm** **FWHM x = 3.54 arcsec** **FWHM y = 1.24 arcsec** **HEW = 3.13 arcsec**

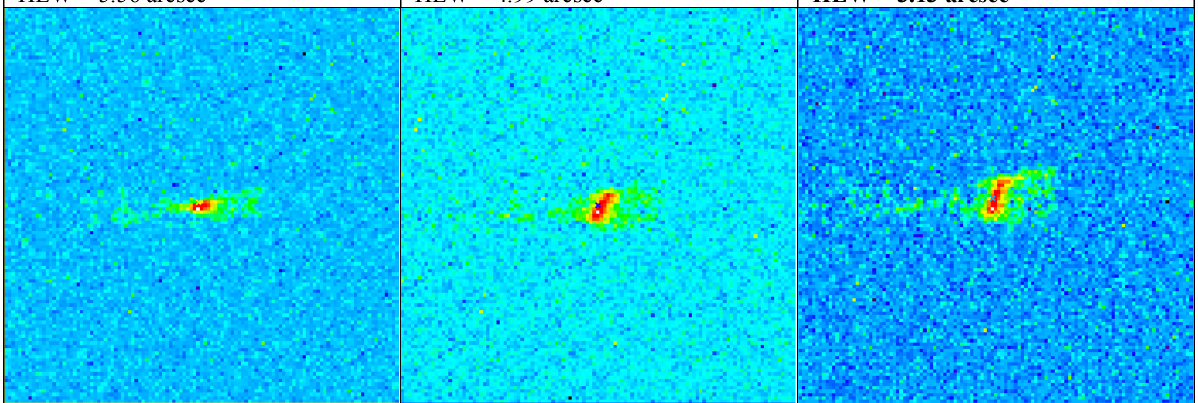

DETQK 154341 steps = -196 mm FWHM x = 3.67 arcsec FWHM y = 1.66 arcsec HEW = 3.55 arcsec	DETQK 162341 steps = -186 mm FWHM x = 3.52 arcsec FWHM y = 5.63 arcsec HEW = 4.22 arcsec	DETQK 166341 steps = -181 mm FWHM x = 3.15 arcsec FWHM y = 7.48 arcsec HEW = 4.79 arcsec

Figure 15: focus search in parallel beam setup at 1.49 keV with PIXI, varying the detector distance from intra- to extra-focal. The best focus is located at -201 mm (intra-focal) wrt the best focus in diverging beam setup (see Figure 5).

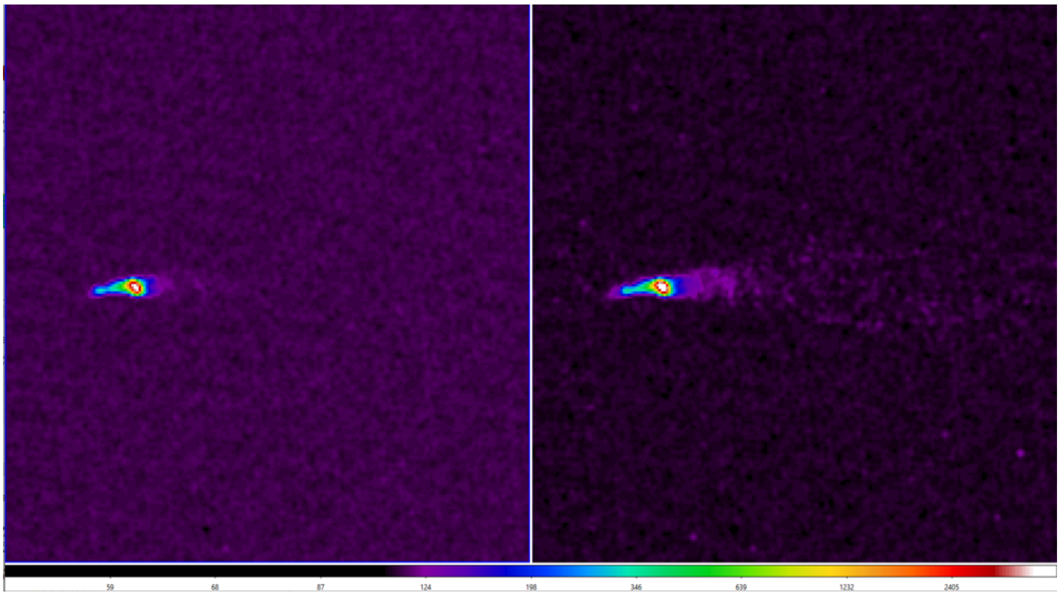

Figure 16: deep exposure in the best focus of the BEaTriX mirror at 1.49 keV, parallel beam setup. (left) median, (right) sum of 8 PIXI images of 5 min exposure time each. The FWHM is close to 3.4 arcsec. Logarithmic color scale.

3.4. Determination of the absolute focal length

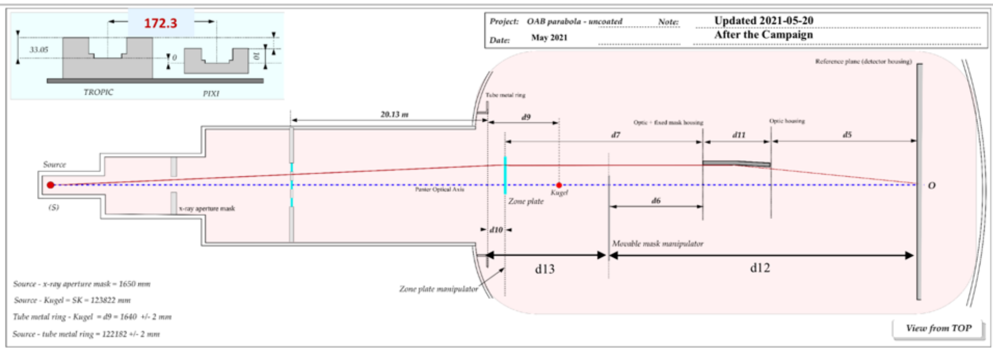

Variable	Calculated Value (mm)	Measured Value – Before (mm)	Measured Value – After (mm)		Comments
			Divergent	Parallel	
d5	4798	4798	4890	4697	Distance from Küche-side of optic to detector housing (4831 mm to TRoPIC chip, average of parallel and divergent beam focus)
d6	TBC	1037		1037	Küche-side of movable mask to Quelle-side of optic+mask
d7	4380	4410		4409	Küche-side of ZP to Quelle-side of optic+mask
d8	9889	9939	10031	9840	Detector stable position (distance from previous campaign)
d9	-	1640 ± 2			Fixed distance
d10	-	280			Fixed distance
d11	456				Physical length of optic from the model
d12		6292	6384	6192	
d13		3644		3653	

Figure 17: distances measured after venting the chamber, with the detector and the mirror still aligned in the best focus position with the parallel beam.

The PIXI detector has been left in the best focal position measured with the parallel beam when the chamber was vented and opened, then the PANTER team has measured the distances reported in Figure 17. The distance d5 (from the physical edge of the mirror to the detector housing) remarkably reads 4697 mm in parallel beam setup. Adding the distance from the housing to the detector surface (33 mm) and half the mirror length (228 mm), one easily gets a total focal length of ***4958 mm***, *in excellent agreement with the nominal value of 4959 mm*, and in accord with the 201 mm of separation measured between the diverging and the parallel focus by PIXI. The measurement of the divergent focus, however, returns a focal length 8 mm shorter than expected, showing that the real focal length is probably a few mm shorter, even if a ±5 mm uncertainty always remains in the absolute focal length determination. The measurements will be repeated on the coated parabola, aiming at a better precision (Sect. 4 and 5).

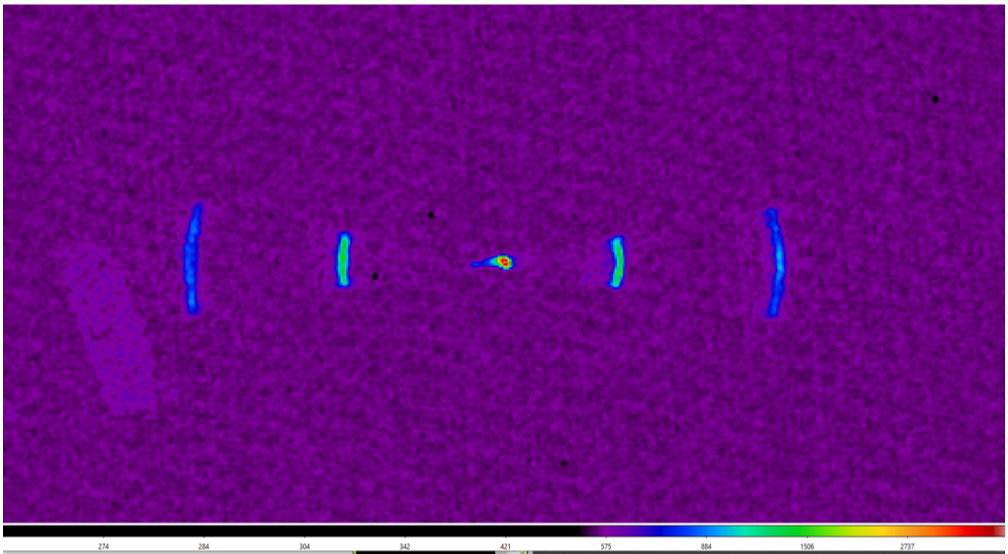

Figure 18: composite image of PIXI exposures, with the best focus changing for mirror pitch steps of 0.5 arcmin. In addition to the spot displacement, we also observe defocusing due to the misalignment.

Another method to determine the absolute focal length goes through the plate scale determination, i.e., the displacement of the focal spot as a function of the mirror pitch rotation; an example is displayed in Figure 18, where the mirror pitch was changed in steps of 0.5 arcmin around the best focus. The lateral displacement (Figure 19) returns a focal length of (5012 ± 88) mm, imprecise but definitely consistent with the previous measurements.

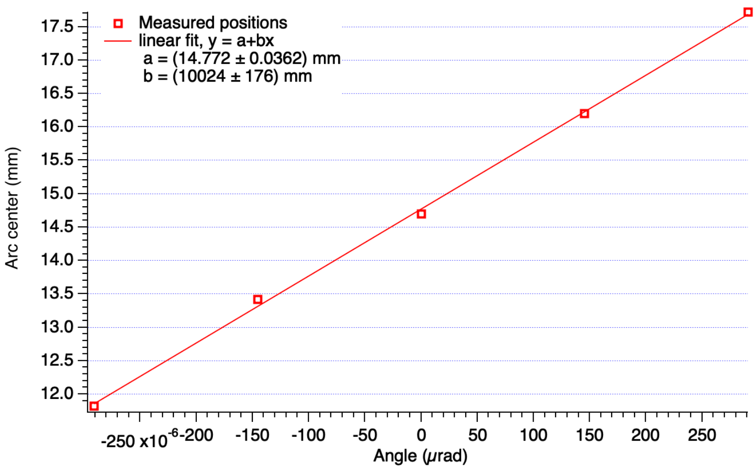

Figure 19: linear fit of the center of the defocused arcs vs. pitch angle misalignments. The estimated focal length is b/2, i.e. (5012 ± 88) mm.

4. Coated mirror under diverging X-ray beam (1.49 keV and 4.51 keV)

After the mirror coating with a 4.6 nm of chromium and 30 nm of platinum at DTU space (Figure 20), the paraboloidal mirror has been brought back to PANTER and re-tested in exactly the same way we did for the uncoated mirror. The alignment procedure, essentially the same suggested in [RD4] and adopted for the uncoated mirror has followed the steps outlined in the dedicated report [RD12]. After an alignment by eye using the laser in the chamber (Figure 21) on the TRoPIC detector at DETQK 322883 steps (4890 mm from mirror center), the alignment has been carried out under diverging beam at 1.49 keV, first adjusting the yaw angle and finding the best upright position for the defocused image. The same procedure was carried out for the alignment in pitch angle (Figure 22), finding at the same time the best focal distance.

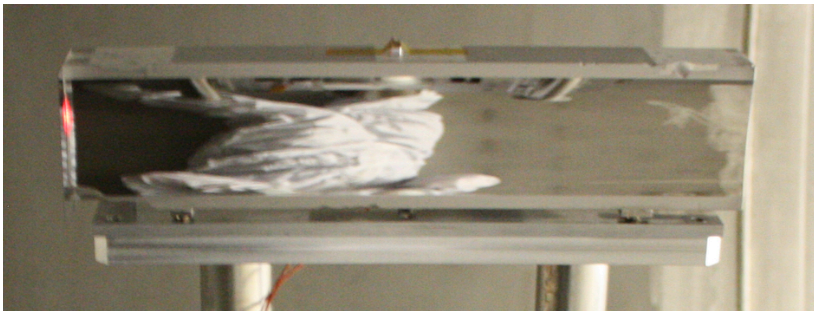

Figure 20: the coated parabola as mounted in the PANTER vacuum chamber (front view).

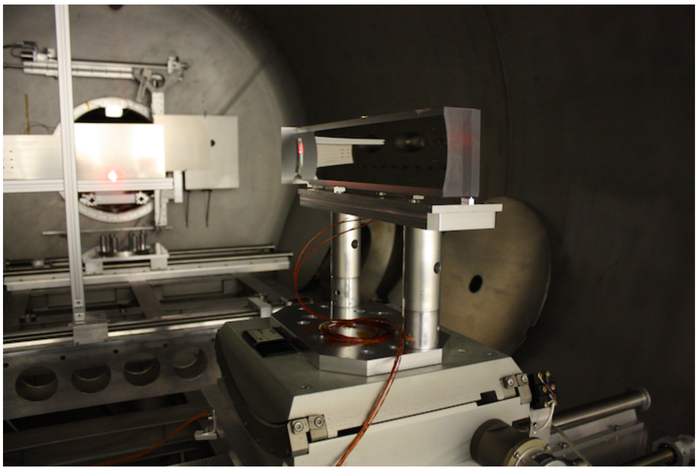

Figure 21: the coated parabola as mounted in the PANTER vacuum chamber. The alignment laser is visible and glaring through the entrance slit.

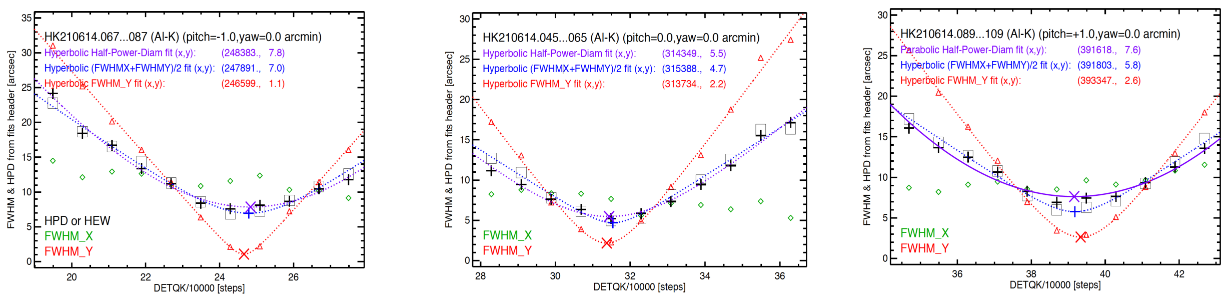

Figure 22: fine alignment of the coated mirror at 1.49 keV under diverging light, searching the focus at different steps of the mirror pitch angle at 1 arcmin steps. The focus displacement is the one expected from simulations.

The best focus under diverging beam at 1.49 keV was actually found 10.7 mm farther than the uncoated mirror one. Due to the uncertainty introduced by the pitch alignment and the focus depth itself (± 5 mm), the variation of 10 mm is still within the uncertainty range of the absolute measurement before coating. The measurements in the best focus, at 1.49 keV and 4.51 keV, are shown in Figure 23.

At 1.49 keV, the focal spot was essentially unchanged with respect to the one before coating (Figure 13*,* left). No increase in scattering can be observed, meaning the surface roughness was not degraded by the deposition of the reflective coating. The HEW value, **5.1 arcsec** measured with TRoPIC, remained the same and also in agreement with the predicted value. The effective area (2.94 ± 0.05) cm^2 was also unchanged within the measurement uncertainty, as expected.

At 4.51 keV, energy of operation for this mirror in BEaTriX, the focal spot exhibits the same shape and overall size, with a larger amount of diffuse scattering. This was also foreseen in the model, even if the impact on the HEW is larger. The measured HEW is **6.36 arcsec**, i.e., a 1.16 arcsec increase with respect to the energy used for alignment, assuming a linear sum of the figure and of the scattering term. The reason for the larger amount of scattering is not fully understood, but it might reveal an underestimation of the mid-frequencies (1 cm – 1 mm) in the metrology tools used. The measured effective area, (1.53 ± 0.03) cm^2, is also lower than the expected value (1.73 cm^2), a reduction of about 11%.

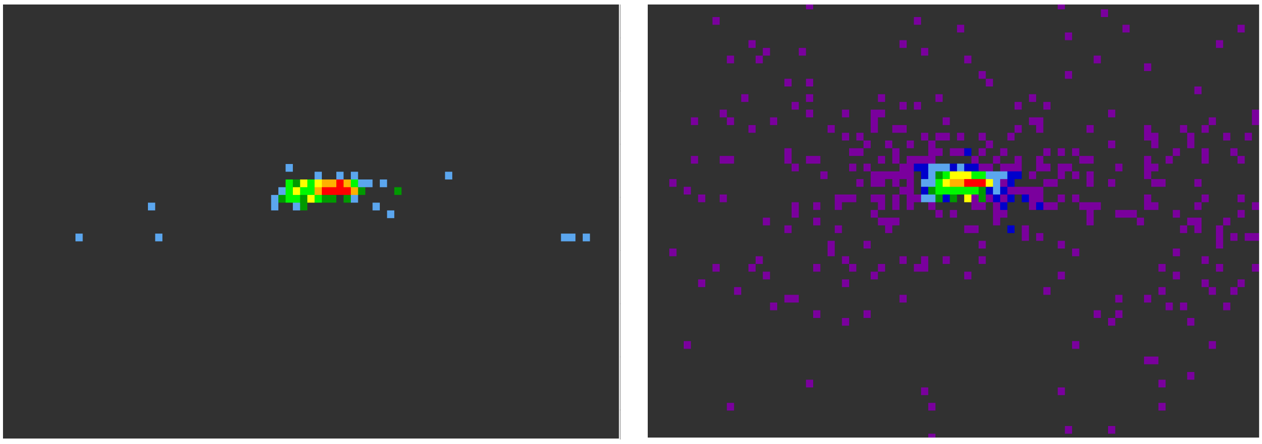

Figure 23: the best focus of the coated mirror in diverging beam setup, seen by TRoPIC. Left: at 1.49 keV, HEW = 5.1 arcsec. Right: at 4.51 keV, HEW = 6.36 arcsec.

Such a decrease in the effective area can hardly be justified on the basis of the excellent smoothness of the coating, which at high frequencies was even improved by the deposition process. Even if some uncertainty can be due to the accuracy of the optical constants of platinum, and the reflectivity thereof, used in the simulation – the incidence angle is not far from the critical angle at 4.51 keV – some insight comes from the out-of-focus images shown in Figure 24 and Figure 25: comparison with the images taken before coating (Figure 8 and Figure 9) show that the surface quality did not significantly change before and after coating. Some scattering increase can be observed, as anticipated, at 4.51 keV along with some increased confusion in the striations parallel to the main curvature of the mirror. The "halo" visible on the two sides seems to come mostly from the two edges, where the optical quality is known to be worse and that should not be illuminated with X-rays. However, some misalignment of the entrance slit to the clear aperture might cause some terminal part to be illuminated and so give rise to larger amounts of scattering at 4.51 keV. These regions will not contribute to the expanded beam in BEaTriX, because they will only marginally be overlapped to the projection of the asymmetric crystal.

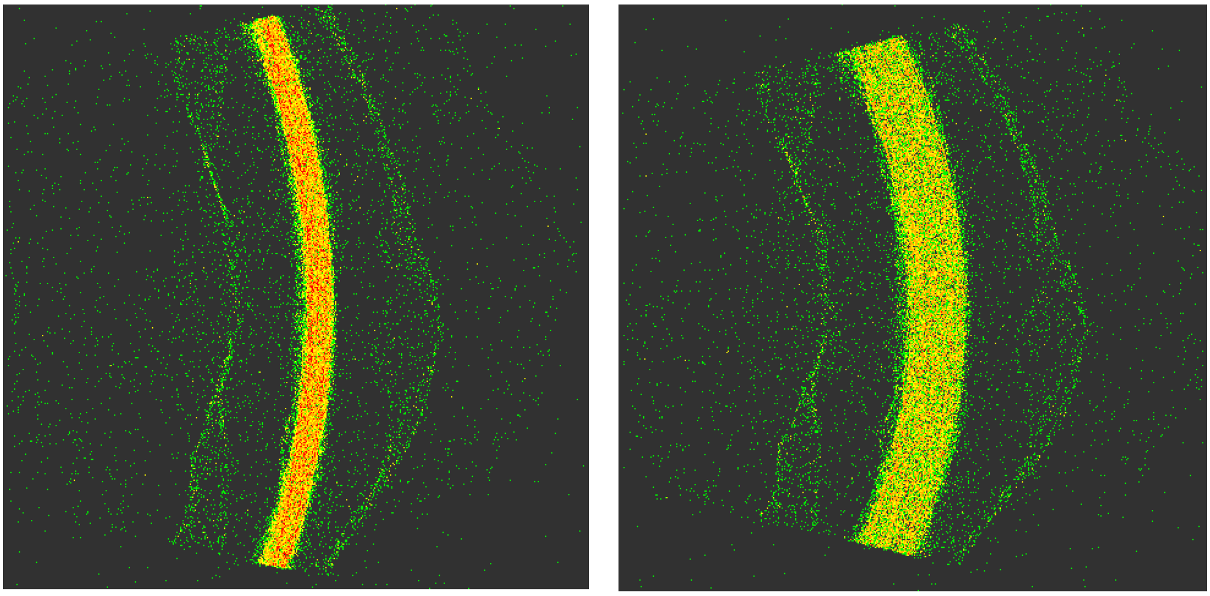

Figure 24: the coated mirror, out-of-focus under diverging X-rays at 1.49 keV. Left: intrafocal image by 384 mm, pitch = + 12.4 arcmin. Right: extrafocal image by 150 mm, pitch = 15.1 arcmin.

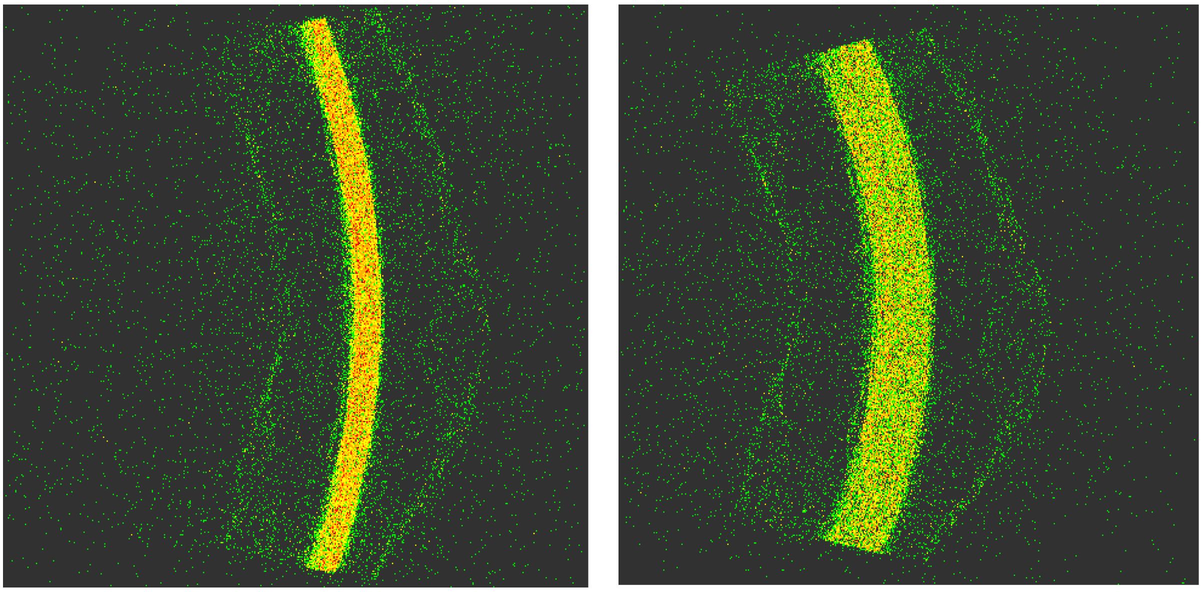

Figure 25: the coated mirror, out-of-focus under diverging X-rays at 4.51 keV. Left: intrafocal image by 384 mm, pitch = + 12.4 arcmin. Right: extrafocal image by 150 mm, pitch = 15.1 arcmin.

5. Coated mirror under parallel X-ray beam (1.49 keV)

For completeness, we have performed the measurement of the BEaTriX mirror under X-rays at 1.49 keV in parallel setup, using the zone plate already utilized for the characterization of the uncoated mirror (Sect. 3). After insertion of the ZP and the selection of the correct diffraction order, the mirror has been re-aligned with PIXI in pitch and yaw angles and focal distance until the minimization of the HEW was reached (Figure 26 and Figure 27). The results (absolute focal length and PSF in the best focus, Figure 28) did not significantly differ from the characterization pre-coating, and possibly showed some improvement at 1.49 keV.

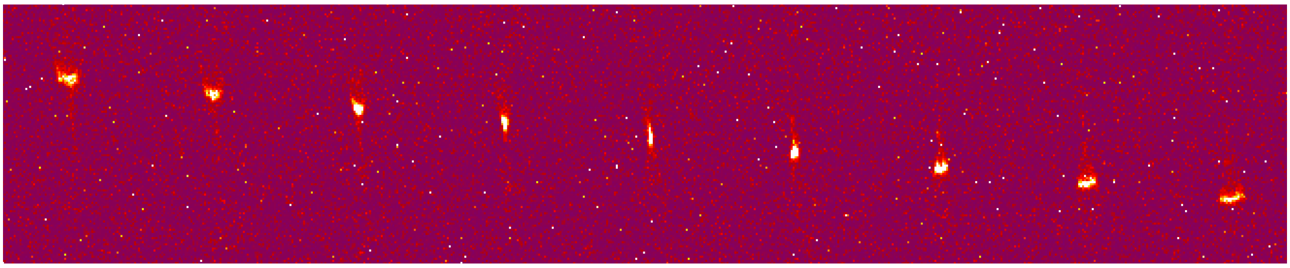

Figure 26: focus search using PIXI under parallel X-rays, at mirror pitch = -0.1 arcmin, after the yaw angle was optimized.

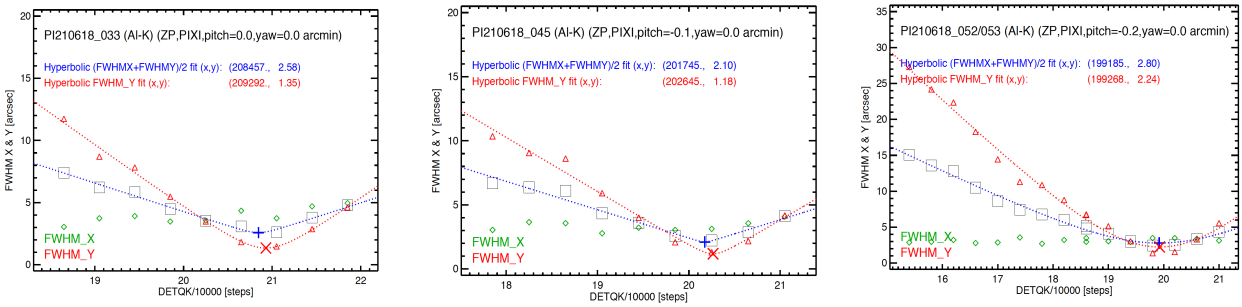

Figure 27: fine alignment of the coated mirror, searching the focus at different steps of the mirror pitch angle.

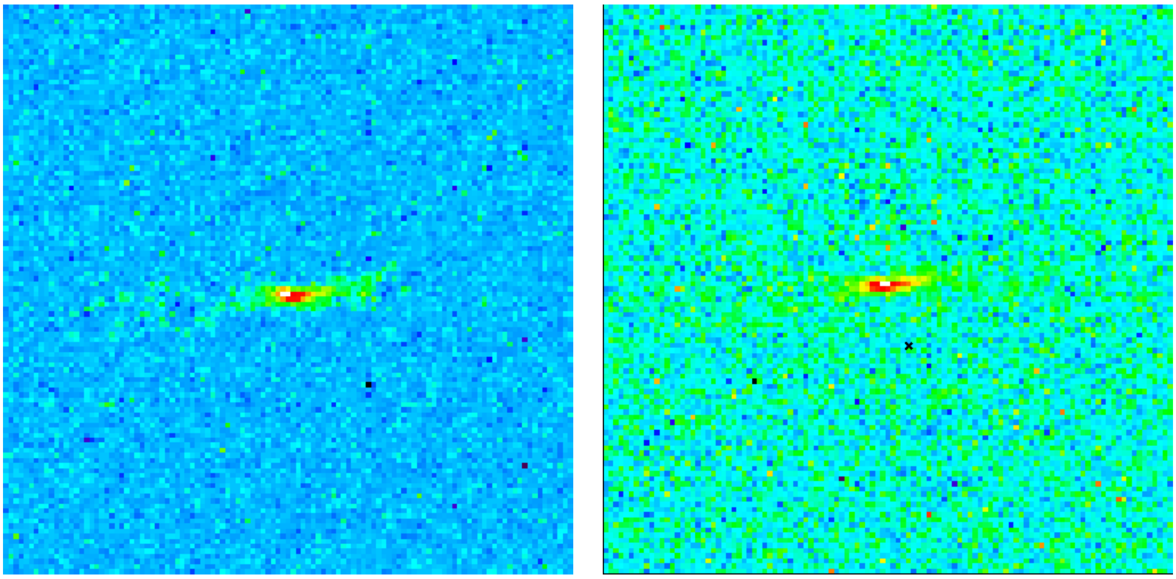

*Figure 28: the best focus of the coated mirror at 1.49 keV in parallel beam setup, as seen by PIXI. Left: before coating, HEW = **3.1 arcsec**. Right: after coating, HEW = **2.8 arcsec**.*

6. Conclusions

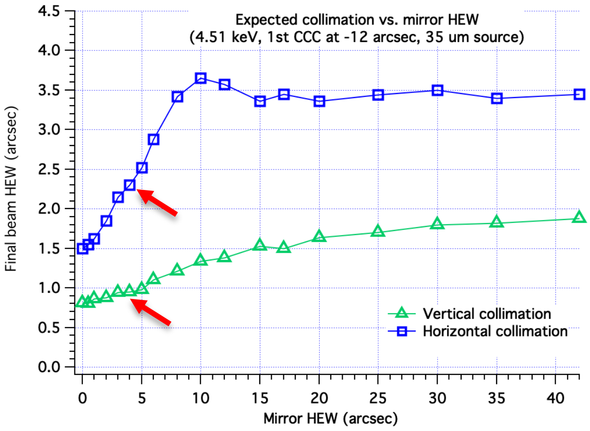

Figure 29: expected vertical and horizontal collimation HEW, based on the measured performances of the coated mirror at 4.51 keV, for the high-energy beamline of BEaTriX.

The measurement campaign pre- and post-coating has enabled the direct characterization of the BEaTriX collimating mirror in X-rays at 1.49 keV. It has confirmed the excellent performance of the mirror, corroborated the metrology characterization, and provided a pathway to the realization of the mirror for the second beamline at 1.49 keV. Due to the lack of a ZP working at 4.51 keV, we could not directly measure the mirror HEW in parallel beam setup, at the energy of operation for the high-energy beamline. The measurement in diverging beam, on the other hand, is affected by the coma aberrations due to the finite distance of the X-ray source. Nevertheless, from the measurement in parallel beam at 1.49 keV post-coating (Sect. 5), which returned 2.8 arcsec, plus the 1.16 arcsec increment of HEW from 1.49 keV to 4.51 keV in diverging beam setup at the best alignment, we can obtain a final result of **HEW= 4 arcsec** as it would be measured in parallel 4.51 keV X-rays. This number assumes a linear sum of geometrical effects and scattering, as already experienced in past campaigns [RD8]. The measurement still includes the size of the X-ray source (< 1 arcsec), so the real HEW of the mirror is probably a bit smaller than 4 arcsec, and essentially in line with the simulations reported in the test plan [RD4].

Anyway, simulations of the full expanded beam of BEaTriX (Figure 29) show that a 4 arcsec HEW is sufficient to return very satisfactory performances of the facility: due to the filtering effect of the monochromators, the final divergence of the expanded beam would be damped to **2.3 arcsec in horizontal and 1 arcsec in vertical** (the latter is solely due to the source size and the azimuthal errors of the mirror, that have a 100 times lesser weight than longitudinal ones). We therefore look forward to mounting the paraboloidal mirror in BEaTriX and perform its alignment to generate the expanded beam soon.